

This Page Is Inserted by IFW Operations
and is not a part of the Official Record

BEST AVAILABLE IMAGES

Defective images within this document are accurate representations of the original documents submitted by the applicant.

Defects in the images may include (but are not limited to):

- BLACK BORDERS
- TEXT CUT OFF AT TOP, BOTTOM OR SIDES
- FADED TEXT
- ILLEGIBLE TEXT
- SKEWED/SLANTED IMAGES
- COLORED PHOTOS
- BLACK OR VERY BLACK AND WHITE DARK PHOTOS
- GRAY SCALE DOCUMENTS

IMAGES ARE BEST AVAILABLE COPY.

**As rescanning documents *will not* correct images,
please do not report the images to the
Image Problem Mailbox.**

(c.f.u.) of V586 was resuspended in 200 µl of TE buffer. Serial dilutions of 1:1, 1:2.5, 1:5, 1:10 and 1:20 were made in TE buffer and 5 µl aliquots representing the DNA concentrations 875 ng, 700 ng, 350 ng, 175 ng and 87.5 ng were subjected to 40 cycles of PCR amplification with the primer pair L1 (5'-GGAGGACTAAGTATCAAGATATT CGTAC-3') and R1 (5'-CAGAAGCTAGCTTATCCCACTAACACAGGA-3'). This primer pair amplifies a 2.4-kb region spanning the deletion site only in strain V583. The lowest concentration of V583 template that resulted in a detectable product under the PCR conditions used was 175 pg of template (equivalent to DNA from approx. 2.2×10^3 c.f.u.). A detectable amplification product of similar intensity was obtained from 175 ng of V586 DNA (equivalent to DNA from approx. 2.2×10^6 c.f.u.), demonstrating that the frequency of deletion of the 17,036-bp DNA segment from V586 is approximately 1 in 10^3 cells.

Quantitative PCR to determine the frequency of deletion of the entire PAI was done essentially as described above using primer pair PAI 64 (5'-ATGCCATGTTTCAGC GAAGTTGCCAATTATC-3') and PAI 167 (5'-GCTGATTATTTATGTTTCTCAGC AATCGCC-3'). The lowest concentration of OGI DNA (which lacks the PAI) that resulted in an amplified product of 2,121 bp was 20 pg (equivalent to DNA from 2×10^2 c.f.u.). No amplified product was detected when up to 2 µg (equivalent to DNA from 2×10^7 c.f.u.) of genomic DNA from V583, V586 or MMH594 was used as template, indicating that deletion of the entire PAI in these strains occurs at a frequency of less than 1 in 10^5 cells.

Received 31 December 2001; accepted 3 April 2002; doi:10.1038/nature00802.

- Richards, M. J., Edwards, J. R., Culver, D. H. & Gaynes, R. P. Nosocomial infections in combined medical-surgical intensive care units in the United States. *Infect. Control Hosp. Epidemiol.* 21, 510–515 (2000).
- Huycke, M. M., Spiegel, C. A. & Gilmore, M. S. Bacteremia caused by hemolytic, high-level gentamicin-resistant *Enterococcus faecalis*. *Antimicrob. Agents Chemother.* 35, 1626–1634 (1991).
- Sahn, D. F. et al. *In vitro* susceptibility studies of vancomycin-resistant *Enterococcus faecalis*. *Antimicrob. Agents Chemother.* 33, 1588–1591 (1989).
- Arthur, M. & Courvalin, P. Genetics and mechanisms of glycopeptide resistance in enterococci. *Antimicrob. Agents Chemother.* 37, 1563–1571 (1993).
- Jett, B. D., Huycke, M. M. & Gilmore, M. S. Virulence of enterococci. *Clin. Microbiol. Rev.* 7, 462–478 (1994).
- Haas, W., Shepard, B. D. & Gilmore, M. S. Two-component regulator of *Enterococcus faecalis* cytotoxicity responds to quorum-sensing autoinduction. *Nature* 415, 84–87 (2002).
- Ike, Y., Hashimoto, H. & Clewell, D. B. Hemolysin of *Streptococcus faecalis* subspecies *zymogenes* contributes to virulence in mice. *Infect. Immun.* 45, 528–530 (1984).
- Shankar, V., Baghdayan, A. S., Huycke, M. M., Lindahl, G. & Gilmore, M. S. Infection-derived *Enterococcus faecalis* strains are enriched in *esp*, a gene encoding a novel surface protein. *Infect. Immun.* 67, 193–200 (1999).
- Shankar, N. et al. Role of *Enterococcus faecalis* surface protein *Esp* in the pathogenesis of ascending urinary tract infection. *Infect. Immun.* 69, 4366–4372 (2001).
- Toledo-Arana, A. et al. The enterococcal surface protein, *Esp*, is involved in *Enterococcus faecalis* biofilm formation. *Appl. Environ. Microbiol.* 67, 4538–4545 (2001).
- Willems, R. J. L. et al. Variant *esp* gene as a marker of a distinct genetic lineage of vancomycin-resistant *Enterococcus faecium* spreading in hospitals. *Lancet* 357, 853–855 (2001).
- Woodford, N., Soltani, M. & Hardy, K. J. Frequency of *esp* in *Enterococcus faecium* isolates. *Lancet* 358, 584 (2001).
- Baldassarri, L., Bertuccini, L., Amendolia, M. G., Gherardi, G. & Creti, R. Variant *esp* gene in vancomycin-sensitive *Enterococcus faecium*. *Lancet* 357, 1802 (2001).
- Rouch, D. A., Byrne, M. E., Kong, Y. C. & Skurray, R. A. The *aacA-aphD* gentamicin and kanamycin resistance determinant of Tn4001 from *Staphylococcus aureus*: expression and nucleotide sequence analysis. *J. Gen. Microbiol.* 133, 3039–3052 (1987).
- Dodd, H. M., Horn, N. & Gasson, M. J. Characterization of IS905, a new multicopy insertion sequence identified in lactococci. *J. Bacteriol.* 176, 3393–3396 (1994).
- Flier, J. & Guiney, D. G. Diverse virulence traits underlying different clinical outcomes of *Salmonella* infection. *J. Clin. Invest.* 107, 775–780 (2001).
- Gold, O. G., Jordan, H. V. & van Houtte, J. The prevalence of enterococci in the human mouth and their pathogenicity in animal models. *Arch. Oral Biol.* 20, 473–477 (1975).
- Ferat, J. L. & Michel, F. Group II self-splicing introns in bacteria. *Nature* 364, 358–361 (1993).
- Huang, C. C., Narita, M., Yamagata, T. & Endo, G. Identification of three *merB* genes and characterization of a broad-spectrum mercury resistance module encoded by a class II transposon of *Bacillus megaterium* strain MB1. *Gene* 239, 361–366 (1999).
- Francia, M. V. et al. Completion of the nucleotide sequence of the *Enterococcus faecalis* conjugative virulence plasmid pAD1 and identification of a second transfer origin. *Plasmid* 46, 117–127 (2001).
- Hacker, J. & Kaper, J. B. Pathogenicity islands and the evolution of microbes. *Annu. Rev. Microbiol.* 54, 641–679 (2000).
- Galli, D. & Wirth, R. Comparative analysis of *Enterococcus faecalis* sex pheromone plasmids identifies a single homologous DNA region which codes for aggregation substance. *J. Bacteriol.* 173, 3029–3033 (1991).
- Rakita, R. M. et al. *Enterococcus faecalis* bearing aggregation substance is resistant to killing by human neutrophils despite phagocytosis and neutrophil activation. *Infect. Immun.* 67, 6067–6075 (1999).
- Rozdzinski, E., Marre, R., Susa, M., Wirth, R. & Muscholl-Silberhorn, A. Aggregation substance-mediated adherence of *Enterococcus faecalis* to immobilized extracellular matrix proteins. *Microb. Pathog.* 30, 211–220 (2001).
- Giard, J. C., Rince, A., Capiaux, H., Auffray, Y. & Hartke, A. Inactivation of the stress-and starvation-inducible *gls24* operon has a pleiotropic effect on cell morphology, stress sensitivity, and gene expression in *Enterococcus faecalis*. *J. Bacteriol.* 182, 4512–4520 (2000).
- Novick, R. P., Schlievert, P. & Ruzin, A. Pathogenicity and resistance islands of staphylococci. *Microb. Infect.* 3, 585–594 (2001).
- Brown, J. S., Gilliland, S. M. & Holden, D. W. A *Streptococcus pneumoniae* pathogenicity island encoding an ABC transporter involved in iron uptake and virulence. *Mol. Microbiol.* 40, 572–585 (2001).
- Sambrook, J., Fritsch, E. F. & Maniatis, T. *Molecular Cloning. A Laboratory Manual* (Cold Spring Harbor Laboratory Press, New York, 1990).

29. Rutherford, K. et al. Artemis: sequence visualization and annotation. *Bioinformatics* 16, 944–945 (2000).

Supplementary Information accompanies the paper on Nature's website (<http://www.nature.com/nature>).

Acknowledgements

This work was supported by grants from the National Institutes of Health, American Heart Association and Research to Prevent Blindness. We thank M. Carson for help with generating the linear map of the pathogenicity island.

Competing interests statement

The authors declare that they have no competing financial interests.

Correspondence and requests for materials should be addressed to N.S. (e-mail: nathan-shankar@uohsc.edu).

Subendothelial retention of atherogenic lipoproteins in early atherosclerosis

Kristina Skålen*†, Marla Gustafsson*†, Ellen Knutsen Rydberg*, Lillemor Mattsson Hultén*, Olov Wiklund*, Thomas L. Innerarity† & Jan Borén*

* Wallenberg Laboratory for Cardiovascular Research, Göteborg University, Göteborg S-41345, Sweden

† Gladstone Institute of Cardiovascular Disease, San Francisco, California 94141-9100, USA

† These authors contributed equally to this work

Complications of atherosclerosis are the most common cause of death in Western societies¹. Among the many risk factors identified by epidemiological studies, only elevated levels of lipoproteins containing apolipoprotein (apo) B can drive the development of atherosclerosis in humans and experimental animals even in the absence of other risk factors². However, the mechanisms that lead to atherosclerosis are still poorly understood. We tested the hypothesis that the subendothelial retention of atherogenic apoB-containing lipoproteins is the initiating event in atherogenesis³. The extracellular matrix of the subendothelium, particularly proteoglycans, is thought to play a major role in the retention of atherogenic lipoproteins⁴. The interaction between atherogenic lipoproteins and proteoglycans involves an ionic interaction between basic amino acids in apoB100 and negatively charged sulphate groups on the proteoglycans⁵. Here we present direct experimental evidence that the atherogenicity of apoB-containing low-density lipoproteins (LDL) is linked to their affinity for artery wall proteoglycans. Mice expressing proteoglycan-binding-defective LDL developed significantly less atherosclerosis than mice expressing wild-type control LDL. We conclude that subendothelial retention of apoB100-containing lipoprotein is an early step in atherogenesis.

Table 1 Mutants of the human apoB100 gene

Recombinant LDL	LDL receptor binding	Proteoglycan binding
Control	Normal	Normal
W ₄₁₆₆ → Y	Defective	Normal
R _{K3359-3362} → S,A	Defective	Defective
K ₃₃₃₃ → E	Normal	Defective
6-GSSM	Defective	Defective

To investigate the potential importance of LDL binding to artery wall proteoglycans in atherogenesis, we created transgenic mice expressing five types of human recombinant LDL (Table 1), fed them an atherogenic diet (1.2% cholesterol, 0.5% cholic acids, and 18% fat) for 20 weeks, and quantitated the extent of atherosclerosis. The first transgenic mouse line expressed human recombinant control LDL⁶. The second transgenic mouse line expressed recombinant LDL with a tyrosine substituted for tryptophan-4369 in apoB100 (W₄₃₆₉ → Y), causing a conformational change that disrupts LDL-receptor binding but does not affect the interaction with proteoglycans⁵. The ability to discriminate between proteoglycan-binding activity and LDL-receptor-binding activity was important because the principal proteoglycan-binding site coincides with the LDL-receptor-binding site in apoB100⁶.

The third transgenic mouse line expressed recombinant LDL in which the basic amino acids in the proteoglycan-binding site of apoB (residues 3359–3369) were converted to neutral amino acids: arginines to serines and lysines to alanines (R,K_{3359–3369} → S,A)⁶. The fourth expressed human recombinant LDL in which lysine 3363 in apoB was changed to glutamic acid (K₃₃₆₃ → E), which severely impairs the interaction with artery wall proteoglycans without affecting LDL-receptor-binding activity⁷.

The fifth line expressed 6-GBSM (six glycosaminoglycan binding sites mutated) LDL, created by mutating the six carboxy-terminal of the eight glycosaminoglycan-binding sequences identified in delipidated apoB100^{7–9}. Although residues 3359–3369 are the primary site for the interaction of native LDL with proteoglycans⁵, modification of the LDL might expose other proteoglycan-binding sites. In all constructs, a leucine was substituted for glutamine-2153 to prevent the formation of apoB48 (ref. 10). This was important because proteoglycan binding site(s) other than those on normal LDL are exposed and physiologically important on apoB48 LDL¹¹.

Next, we clarified whether proteoglycan-binding-defective LDL undergo normal non-receptor-mediated transcytosis across the endothelium^{1,12} and compared their subendothelial retention *in vivo* with that of control LDL. R,K_{3359–3369} → S,A and recombinant control LDL were labelled with ¹²⁵I and injected into the tail vein of 8-week-old mice. After 20 min or 72 h, the mice were perfusion fixed, and the aortas were dissected and measured for radioactivity. Analysis of aortas 20 min after injection of 5 × 10⁸ c.p.m. of ¹²⁵I-LDL showed no difference in the arterial permeability of the R,K_{3359–3369} → S,A LDL and the control LDL (not shown). However, 72 h after injection of 1 × 10⁷ c.p.m. of ¹²⁵I-LDL, more radioactivity was present in the aortas of mice injected with control LDL than of those injected with proteoglycan-binding-defective LDL (263 ± 117 versus 701 ± 324 c.p.m.; mean ± s.d.; n = 3 per group). Thus, proteoglycan-binding-defective LDL are retained less efficiently than recombinant control LDL in the artery wall *in vivo*.

To determine if elevated levels of proteoglycan-binding-defective LDL would be less atherogenic than similar levels of wild-type recombinant LDL, transgenic mice expressing the five types of human recombinant LDL were fed the atherogenic diet for 20 weeks. The lipoprotein profiles (Fig. 1) and the cholesterol levels were similar in all groups (Table 2), except for the mice expressing R,K_{3359–3369} → S,A LDL and particularly those expressing

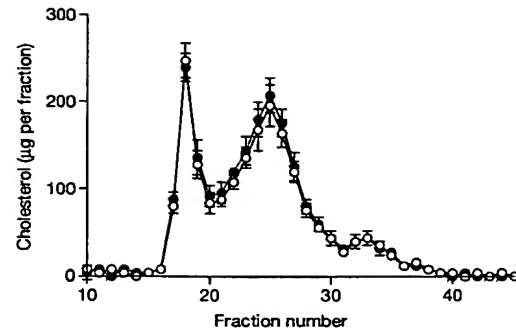


Figure 1 Distribution of cholesterol. Data was assessed by Superose 6 chromatography of pooled plasma from five female human-apoB transgenic mice expressing recombinant control low-density lipoproteins (LDL) (filled circles) or 6-GBSM LDL (open circles) after 20 weeks on an atherogenic diet. Very-low-density lipoproteins correspond to fractions 16–20, LDL to fractions 21–29, and high-density lipoproteins to fractions 30–36.

K₃₃₆₃ → E LDL, which had a lower plasma LDL-cholesterol level owing to lower transgene copy number.

After 20 weeks, 231 mice were perfusion-fixed. Seven aortas were not analysed for technical reasons. The remaining 224 aortas were analysed with the *en face* procedure¹³. The extent of atherosclerosis correlated with the plasma concentration of human apoB100 in all groups (Fig. 2). However, transgenic mice expressing proteoglycan-binding-defective LDL (R,K_{3359–3369} → S,A, 6-GBSM, and K₃₃₆₃ → E LDL) had significantly less atherosclerosis than mice expressing wild-type control or W₄₃₆₉ → Y LDL (Table 3) (*P* < 0.01). Nontransgenic littermate controls (*n* = 5 per group) had essentially no atherosclerosis (not shown). However, plasma concentrations of human apoB100 were lower in mice expressing R,K_{3359–3369} → S,A LDL and K₃₃₆₃ → E LDL than in those expressing recombinant control LDL, so W₄₃₆₉ → Y LDL or 6-GBSM LDL (Table 2). We also calculated 95% Boole-Bonferroni simultaneous confidence intervals (99% individual confidence degrees) for each of the five regression slopes, individually. The intervals for the regression slopes of recombinant control LDL and W₄₃₆₉ → Y LDL did not overlap with those of the three groups of proteoglycan-binding-defective LDL. This finding confirms the pairwise differences in the amount of atherosclerosis between the groups.

These results strongly indicate that proteoglycan-binding-defective LDL have a greatly reduced atherogenic potential and provide direct experimental evidence that direct binding of LDL to artery wall proteoglycans is a key step in atherogenesis.

To verify that the differences in atherogenicity were due solely to different affinities for arterial proteoglycans, we performed several control experiments. First, we analysed the formation of conjugated dienes in R,K_{3359–3369} → S,A LDL and recombinant control LDL after copper-stimulated oxidation¹⁴. The lag phase for the formation of conjugated dienes in R,K_{3359–3369} → S,A LDL and recombinant control LDL was 79 ± 6 and 74 ± 8 min, respectively, and the

Table 2 Lipid, lipoprotein and apoB measurements in transgenic mice expressing recombinant LDL

	Control LDL	W ₄₃₆₉ → Y LDL	R,K _{3359–3369} → S,A LDL	K ₃₃₆₃ → E LDL	6-GBSM LDL
Total cholesterol	8.49 ± 0.97	8.43 ± 1.02	7.32 ± 0.92*	5.19 ± 0.64*	9.17 ± 0.90
HDL cholesterol	0.78 ± 0.06	0.76 ± 0.05	0.77 ± 0.04	0.79 ± 0.03	0.75 ± 0.05
Triglyceride	0.18 ± 0.016	0.17 ± 0.014	0.18 ± 0.015	0.19 ± 0.020	0.18 ± 0.013
Human apoB100	2,334 ± 59	2,326 ± 67	1,935 ± 55*	1,424 ± 41*	2,518 ± 61

Plasma lipid and lipoprotein (nmol l⁻¹) and apoB levels (µg ml⁻¹) in female mice after 20 weeks on an atherogenic diet. Values are mean ± s.e.m. (*n* = 20 per group, except for human apoB100, where *n* = 40 per group).

**P* < 0.001 versus control LDL.

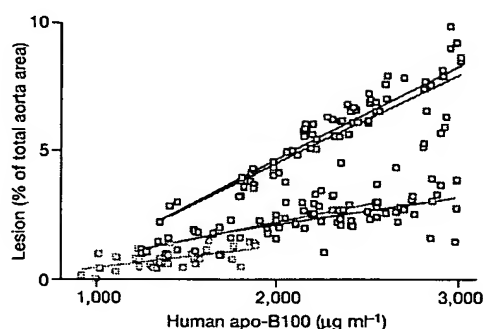


Figure 2 Effect on aorta of an atherogenic diet in transgenic mice. The data shows the correlation between the percentage of total aortic surface area covered by lesions and the plasma concentration of human apoB100 in transgenic mice fed an atherogenic diet for 20 weeks. Recombinant control LDL (red) and $W_{4369} \rightarrow Y$ LDL (blue), both with normal proteoglycan binding. Proteoglycan-binding-defective $R_{K3359-3369} \rightarrow S,A$ LDL (pink), $K_{3363} \rightarrow E$ LDL (light green), and 6-GBSM LDL (dark green). The percentage of total aortic surface area covered by lesions in mice expressing the recombinant LDL were 5.7 ± 1.5 , 5.8 ± 1.7 , 2.1 ± 0.66 , 0.81 ± 0.36 or 2.7 ± 0.72 , respectively (mean \pm s.d.).

maximal rate of conjugated dienes formed was 6.1 ± 0.5 and 5.8 ± 0.4 molecules $\text{min}^{-1} \times \text{LDL}$ particle, respectively (mean \pm s.d.; $n = 3$). Thus, proteoglycan-binding-defective LDL were as susceptible to oxidation as recombinant control LDL.

Next, we incubated minimally oxidized LDL with human and mouse macrophages and analysed the inflammatory response. After incubation with human monocyte-derived macrophages for 24 h, the TNF α concentrations in cell-culture media containing minimally oxidized $R_{K3359-3369} \rightarrow S,A$ LDL or recombinant control LDL were not significantly different (42.2 ± 12.5 and 37.2 ± 10.3 pg per ml medium; mean of duplicate measurements of macrophages from two donors analysed separately). Similarly, after incubation with minimally oxidized $R_{K3359-3369} \rightarrow S,A$ LDL or recombinant control LDL for 24 h, bone-marrow derived macrophages from transgenic mice expressing an NF κ B-luciferase reporter gene showed no differences in luciferase activity (mean \pm s.d., 435 ± 36 and 458 ± 64 relative light units per $10 \mu\text{g}$ protein, respectively; $n = 4$). The concentrations of thiobarbituric-acid-reactive substances¹⁵ (TBARS), lipid hydroperoxide (LPO), and hydrogen peroxide were the same in the minimally oxidized $R_{K3359-3369} \rightarrow S,A$ LDL and the minimally oxidized recombinant control LDL (15 ± 3.5 versus 12.5 ± 4.0 nmol MDA per-mg LDL, 252 ± 45 versus 225 ± 32 nmol per mg LDL, and 2.51 ± 0.85 versus 3.63 ± 1.2 nmol per mg LDL, respectively).

To exclude differences in binding and uptake of proteoglycan-binding-defective LDL and recombinant control LDL in macrophages, LDL were radiolabelled with ^{125}I and incubated with human monocyte-derived macrophages for 6 or 24 h. There were no differences in the binding or uptake of recombinant control or proteoglycan-binding-defective LDL (Table 3). We also analysed the

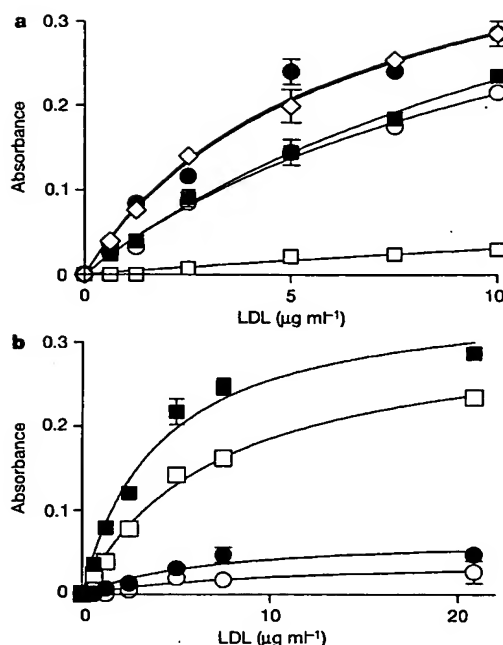


Figure 3 Plate-assay analysis of the ability of recombinant LDL to interact with biglycan. **a.** Recombinant control LDL from $Ldlr^{-/-}$ mice (filled circles) or $Ldlr^{+/+}$ mice (open circles), recombinant $R_{K3359-3369} \rightarrow S,A$ LDL from $Ldlr^{-/-}$ mice (filled squares) or $Ldlr^{+/+}$ mice (open squares), or human plasma LDL (diamonds). **b.** Recombinant $R_{K3359-3369} \rightarrow S,A$ LDL from $Ldlr^{-/-}$ mice (open squares), recombinant $R_{K3359-3369} \rightarrow S,A$ LDL from $Ldlr^{+/+}$ mice with CHD-modified human apoE (open circles), or human plasma LDL (filled squares). CHD-modified human plasma LDL (filled circles) were included as a negative control. The recombinant lipoproteins were isolated from ten mice each, and endogenous apoB was removed by immunoaffinity chromatography.

accumulation of ^{14}C -cholesterol esters in macrophages incubated with $R_{K3359-3369} \rightarrow S,A$ LDL or recombinant control LDL isolated from mice injected with $[1,2-^{14}\text{C}]$ acetate. The macrophages accumulated similar amounts of ^{14}C -cholesterol esters after being incubated with radiolabelled $R_{K3359-3369} \rightarrow S,A$ LDL or recombinant control LDL for 24 h ($1,193 \pm 263$ versus $1,274 \pm 382$ c.p.m. per mg cell protein, respectively; mean \pm s.d. of duplicate measurements on macrophages from six donors analysed separately).

Finally, mice expressing $R_{K3359-3369} \rightarrow S,A$ LDL or recombinant control LDL were bred onto the LDL-receptor-null background ($Ldlr^{-/-}$). Because apoE is a ligand for the LDL receptor, the recombinant LDL in $Ldlr^{-/-}$ mice become enriched in apoE. ApoE also facilitates an indirect interaction between LDL and artery wall proteoglycans¹⁶. Therefore, if the decreased atherosclerotic potential of proteoglycan-binding-defective LDL were due solely to its inability to interact with artery wall proteoglycans,

Table 3 Binding and degradation of ^{125}I -LDL to human monocyte-derived macrophages

	Membrane-bound LDL		Intracellular LDL		Degraded LDL	
Hours incubated	6	24	6	24	6	24
Human LDL	288 \pm 37	598 \pm 295	709 \pm 59	1,543 \pm 185	1,535 \pm 21	3,857 \pm 1,031
Control LDL	380 \pm 23	787 \pm 549	858 \pm 4	1,822 \pm 344	1,563 \pm 14	5,381 \pm 1,802
$W_{4369} \rightarrow Y$ LDL	282 \pm 63	721 \pm 503	837 \pm 1	1,824 \pm 418	2,033 \pm 28	4,775 \pm 1,156
$R_{K3359-3369} \rightarrow S,A$ LDL	290 \pm 76	845 \pm 720	835 \pm 80	1,762 \pm 761	1,829 \pm 333	4,340 \pm 1,061
$K_{3363} \rightarrow E$ LDL	242 \pm 36	812 \pm 531	781 \pm 75	1,830 \pm 407	1,834 \pm 207	4,882 \pm 1,351
6-GBSM LDL	367 \pm 157	725 \pm 442	798 \pm 122	1,814 \pm 393	1,748 \pm 478	5,068 \pm 1,050

Macrophages were incubated in medium containing ^{125}I -labelled LDL for 6 or 24 h. Membrane-bound, cell-associated, and degraded LDL were measured and expressed as ng LDL per mg cell protein. Values are mean \pm s.d. of triplicate measurements on macrophages from five donors (for 24 h) or two donors (for 6 h), analysed separately. No significant differences were found between recombinant proteoglycan-binding LDL and proteoglycan-binding-defective LDL (paired Student's *t*-test).

enrichment in apoE would restore its atherogenicity.

Recombinant wild-type control LDL and R_{K3359-3369} → S_A LDL from *Ldlr*^{+/+} or *Ldlr*^{-/-} mice were subjected to plate-assay analysis with biglycan. R_{K3359-3369} → S_A LDL from *Ldlr*^{-/-} mice (that is, apo-E enriched proteoglycan-binding-defective LDL) interacted normally with biglycan, whereas R_{K3359-3369} → S_A LDL from *Ldlr*^{+/+} mice displayed severely defective binding to biglycan (Fig. 3a). These results were verified in binding experiments with the total proteoglycan fraction from aortic smooth muscle cells (not shown).

To confirm the role of apoE in binding to proteoglycans, we incubated R_{K3359-3369} → S_A LDL from *Ldlr*^{-/-} mice with a 200-fold molar excess of cyclohexanedione (CHD)-modified apoE isolated from human very-low-density lipoprotein¹⁷. In two independent experiments, replacement of the endogenous apoE with CHD-modified human apoE abolished the binding to biglycan (Fig. 3b). We also analysed the binding affinity of R_{K3359-3369} → S_A LDL isolated from *Ldlr*^{-/-} or *ApoE*^{-/-} mice. ApoE-enriched R_{K3359-3369} → S_A LDL from *Ldlr*^{-/-} mice bound biglycan with high affinity ($128 \pm 21\%$ of control LDL), whereas apoE-depleted R_{K3359-3369} → S_A LDL from *ApoE*^{-/-} mice displayed severely defective binding ($6 \pm 3\%$ of control LDL).

To determine whether apoE enrichment increases the atherogenicity of proteoglycan-binding-defective R_{K3359-3369} → S_A LDL, we performed atherosclerosis studies in 6-month-old mice. *Ldlr*^{-/-} mice expressing R_{K3359-3369} → S_A LDL or recombinant control LDL developed the same amount of atherosclerosis in both the proximal aortic root (15.8 ± 6.2 and $14.0 \pm 4.6\%$ fraction area of lesion, respectively) and distal aorta (4.54 ± 1.31 and $3.94 \pm 0.89\%$ of total aorta area, respectively). Thus, the reduced atherogenicity of proteoglycan-binding-defective LDL is dependent on its lower affinity for artery-wall proteoglycans, and the reduced atherogenicity can be restored by apoE enrichment. The lipoprotein profiles (not shown) and the plasma cholesterol levels were similar in transgenic *Ldlr*^{-/-} mice expressing recombinant control LDL or R_{K3359-3369} → S_A LDL (mean \pm s.e.m., 15.5 ± 1.3 and 14.7 ± 1.1 mmol l⁻¹, respectively; $n = 0$).

Recombinant LDL from *Ldlr*^{-/-} mice contained approximately 10-fold more apoE than recombinant LDL from *Ldlr*^{+/+} mice. Likewise, the atherogenic diet duplicated the amount of apoE on the recombinant LDL in *Ldlr*^{+/+} mice. The explanation for this is probably a diet-induced down-regulation of LDL receptors. Therefore, proteoglycan-binding-defective LDL from *Ldlr*^{+/+} mice displayed significantly more proteoglycan-binding activity when mice were fed the atherogenic versus the chow (normal food) diet ($29 \pm 6\%$ and $9 \pm 5\%$ of control LDL, respectively). Recombinant control LDL and R_{K3359-3369} → S_A LDL showed identical apoE enrichment after high-fat feeding, and when bred into *Ldlr*^{-/-} mice.

Mouse LDL often contain apoE, but apoB100 is the sole apolipoprotein on human LDL. Thus, bridging molecules are probably less important than a direct interaction between apoB100 and proteoglycans for subendothelial retention of atherogenic lipoproteins in humans. Retained lipoproteins can directly or indirectly provoke all known features of early lesions and, by stimulating local synthesis of proteoglycans, can accelerate further retention and aggregation³. Thus, atherosclerosis is initiated by subendothelial retention of atherogenic lipoproteins. □

Methods

Human apo-B transgenic mice

The human apoB transgenic mice were back-crossed for three generations with C57BL/6 mice or for five generations with *Ldlr*^{-/-} mice on C57BL/6 background (Jackson Laboratory). Mice expressing an NFκB-luciferase reporter gene were a gift from H. Carlsen and R. Blomhoff.

Plasma lipid and lipoprotein measurements

The plasma concentrations of human apoB100 were measured by enzyme-linked

immunosorbent assay (ELISA) using the antihuman apoB antibody 1D1¹⁸ and a horseradish peroxidase (HRP)-conjugated polyclonal antihuman apoB antibody (The Binding Site). The distribution of lipids within the plasma lipoprotein fractions was assessed by fast-performance liquid chromatography (FPLC) gel filtration using a Superose 6 HR 10/30 column (Pharmacia)¹⁹.

Plate-assay analysis with biglycan

Maxisorp immunoplates (NUNC) were coated with biglycan ($10 \mu\text{g ml}^{-1}$) in HEPES-buffered saline (HBS) (20 mM HEPES, 150 mM NaCl, pH 7.4) overnight at room temperature (RT, 22 °C), and blocked with HBS with 1% bovine serum albumin (BSA) for 1 h at RT. The samples of LDL in HBS buffer with 2 mM CaCl₂ and 2 mM MgCl₂ were added to the wells, and incubated for 1 h at RT. The plates were then incubated with the same buffer supplemented with lipoprotein-deficient serum (diluted 1:50) for 30 min. To each well, 100 μl of a HRP-conjugated polyclonal antibody against human apoB (The Binding Site) (diluted 1:750 in HBS with 0.1% BSA and 0.02% Tween 20) was added and incubated at RT for 1.5 h. Finally, 100 μl of Turbo TMB-ELISA (Pierce) substrate was added and incubated for 5 min.

Analysis of atherosclerotic lesions in the proximal aortic root

The heart and 1 mm of the thoracic aorta were embedded in OCT Tissue-Tec medium (Histolab), frozen in dry ice and isopentane, cut into 10- μm -thick cross-sections, and stained in 0.5% Oil Red O². The fraction area of lesion was calculated by dividing the surface of the lesion by the surface of the vessel. This corrects for errors caused by oblique sections²⁰.

Competition of mouse apoE with chemically modified human apoE

Recombinant R_{K3359-3369} → S_A LDL was isolated⁷ and incubated with a 200-fold molar excess of CHD-modified apoE from human very-low-density lipoproteins²¹. The free apoE was removed from the recombinant LDL by ultracentrifugation⁷ ($d = 1.063 \text{ g ml}^{-1}$). The top 1 ml was recovered and separated on a Superose 6 HR 10/30 column. The CHD-modified samples were incubated with an equal volume of 1 M hydroxylamine, 0.3 M mannitol, pH 7.0, at 37 °C for 16 h to reverse the modification of the arginine residues before gel electrophoresis.

Monitoring LDL oxidation

LPO was quantitated with the Lipohydrox kit (Wak-Chemie Medical, Germany). The H₂O₂ content was measured with the Bioxytech H₂O₂-560 assay (Oxis International, USA).

Macrophage preparation

Human monocyte-derived macrophages, prepared separately from buffy coats (lymphocyte fraction of whole blood) from five donors and obtained from Swedish blood banks, were isolated as described²².

Uptake and degradation of LDL

Human LDL and recombinant mouse LDL were labelled with ¹²⁵I (Amersham International) to a specific activity of 46–54 c.p.m. ng⁻¹ (ref. 23). Macrophages were incubated in medium with ¹²⁵I-labelled LDL ($50 \mu\text{g ml}^{-1}$) for 6 or 24 h. The membrane-bound, the cell-associated and the degraded LDL were determined²⁴, and expressed as ng LDL per mg cell protein. In another experiment, mice expressing recombinant control LDL or R_{K3359-3369} → S_A LDL were injected intravenously with 80 μCi [^{1,2-¹⁴C}]acetate (Amersham International) 3, 5 and 10 days before the mice were sacrificed and the recombinant LDL isolated⁷. Macrophages were incubated with ¹⁴C-labelled LDL ($50 \mu\text{g ml}^{-1}$) for 24 h. Lipids were extracted from the cells²⁵, and the radioactivity in ¹⁴C-cholesterol esters was measured after separation by thin-layer chromatography (Silica Gel G) in hexane-diethylether-glacial acetic acid (80:20:1 v/v).

Measurement of TNFα secretion in human macrophages

Human macrophages were cultured for 6 days in RPMI 1640 medium (Bio Whittaker) with 10% human serum and 10% FCS. Macrophages were then incubated for 24 h in serum-free medium containing human or recombinant minimally modified LDL ($100 \mu\text{g ml}^{-1}$). The medium concentration of TNFα was measured by high-sensitivity ELISA for TNFα (R&D Systems) and correlated to cell protein content.

Luciferase measurement in bone-marrow-derived mouse macrophages

Bone-marrow-derived mouse macrophages were isolated from the femurs of female NFκB-luciferase reporter mice²⁶ and seeded at 1×10^6 cells ml⁻¹ in RPMI 1640 containing 10% fetal bovine serum (FBS) and 10% L-cell conditioned medium²⁷. Nonadherent cells were removed 24 h later, resuspended at the same density in fresh medium, and cultured for 6 days until confluence was reached. The mouse macrophages were then incubated for 24 h in serum-free medium containing minimally modified human or recombinant LDL ($100 \mu\text{g ml}^{-1}$). Luciferase activity (Luciferase Assay System, Promega) was determined and normalized for protein content.

Retention of LDL in vivo

Recombinant control LDL and R_{K3359-3369} → S_A LDL were isolated⁷ and radiolabelled with ¹²⁵I using Iodogen (Pierce)²⁸. The specific activity of the recombinant control ¹²⁵I-LDL and the R_{K3359-3369} → S_A ¹²⁵I-LDL was 300 c.p.m. ng⁻¹.

Statistical analysis

Differences in atherosclerosis and lipid levels were assessed by analysis of variance (ANOVA) on ranks and multiple comparison analysis.

Received 6 December 2001; accepted 20 February 2002; doi:10.1038/nature00804.

- Ross, R. Cell biology of atherosclerosis. *Annu. Rev. Physiol.* 57, 791–804 (1995).
- Glass, C. K. & Witztum, J. L. Atherosclerosis. The Road Ahead. *Cell* 104, 503–516 (2001).
- Williams, K. J. & Tabas, I. The response-to-retention hypothesis of early atherogenesis. *Arterioscler. Thromb. Vasc. Biol.* 15, 551–561 (1995).
- Srinivasan, S. R. et al. Low density lipoprotein retention by aortic tissue. Contribution of extracellular matrix. *Atherosclerosis* 62, 201–208 (1986).
- Boren, J. et al. Identification of the principal proteoglycan-binding site in LDL. A single-point mutation in apo-B100 severely affects proteoglycan interaction without affecting LDL receptor binding. *J. Clin. Invest.* 101, 2658–2664 (1998).
- Boren, J. et al. Identification of the low density lipoprotein receptor-binding site in apolipoprotein B100 and the modulation of its binding activity by the carboxyl terminus in familial defective apo-B100. *J. Clin. Invest.* 101, 1084–1093 (1998).
- Weisgraber, K. H. & Ball, S. C. Jr Human apolipoprotein B-100 heparin-binding sites. *J. Biol. Chem.* 262, 11097–11103 (1987).
- Hirose, N., Blankenship, D. T., Krivanek, M. A., Jackson, R. L. & Cardin, A. D. Isolation and characterization of four heparin-binding cyanogen bromide peptides of human plasma apolipoprotein B. *Biochemistry* 26, 5505–5512 (1987).
- Camejo, G., Olofsson, S. O., Lopez, F., Carlsson, P. & Bondjers, G. Identification of Apo B-100 segments mediating the interaction of low density lipoproteins with arterial proteoglycans. *Arteriosclerosis* 8, 368–377 (1988).
- Yao, Z. et al. Elimination of apolipoprotein B48 formation in rat hepatoma cell lines transfected with mutant human apolipoprotein B cDNA constructs. *J. Biol. Chem.* 267, 1175–1182 (1992).
- Goldberg, I. J. et al. The NH2-terminal region of apolipoprotein B is sufficient for lipoprotein association with glycosaminoglycans. *J. Biol. Chem.* 273, 35355–35361 (1998).
- Simionescu, M. & Simionescu, N. Endothelial transport of macromolecules: transcytosis and endocytosis. A look from cell biology. *Cell Biol. Rev.* 25, 5–78 (1991).
- Tangirala, R. K., Rubin, E. M. & Palinski, W. Quantitation of atherosclerosis in murine models: Correlation between lesions in the aortic origin and in the entire aorta, and differences in the extent of lesions between sexes in LDL receptor-deficient and apolipoprotein E-deficient mice. *J. Lipid Res.* 36, 2320–2328 (1995).
- Puhl, H., Waeg, G. & Esterbauer, H. Methods to determine oxidation of low-density lipoproteins. *Methods Enzymol.* 233, 425–441 (1994).
- Yagi, K. A simple fluorometric assay for lipoperoxide in blood plasma. *Biochem. Med.* 15, 212–216 (1976).
- Ji, Z. S., Pitas, R. E. & Mahley, R. W. Differential cellular accumulation/retention of apolipoprotein E mediated by cell surface heparan sulfate proteoglycans. Apolipoproteins E3 and E2 greater than E4. *J. Biol. Chem.* 273, 13452–13460 (1998).
- Brissette, L., Roach, P. D. & Noel, S. P. The effects of liposome-reconstituted apolipoproteins on the binding of rat intermediate density lipoproteins to rat liver membranes. *J. Biol. Chem.* 261, 11631–11638 (1986).
- Milne, R. W., Theolis, R. Jr, Verdery, R. B. & Marcel, Y. L. Characterization of monoclonal antibodies against human low density lipoprotein. *Arteriosclerosis* 3, 23–30 (1983).
- Purcell-Huynh, D. A. et al. Transgenic mice expressing high levels of human apolipoprotein B develop severe atherosclerotic lesions in response to a high-fat diet. *J. Clin. Invest.* 95, 2246–2257 (1995).
- Nicoletti, A., Kaveri, S., Caligiuri, G., Bariety, J. & Hansson, G. K. Immunoglobulin treatment reduces atherosclerosis in apo E knockout mice. *J. Clin. Invest.* 102, 910–918 (1998).
- Mahley, R. W. et al. Inhibition of lipoprotein binding to cell surface receptors of fibroblasts following selective modification of arginyl residues in arginine-rich and B apoproteins. *J. Biol. Chem.* 252, 7279–7287 (1977).
- Ohlsson, B. G. et al. Oxidized low density lipoprotein inhibits lipopolysaccharide-induced binding of nuclear factor-kappaB to DNA and the subsequent expression of tumour necrosis factor- α and interleukin-1 β in macrophages. *J. Clin. Invest.* 98, 78–89 (1996).
- McFarlane, A. S. Efficient trace-labelling of proteins with iodine. *Nature* 182, 53 (1958).
- Hurt-Camejo, E. et al. Effect of arterial proteoglycans and glycosaminoglycans on low density lipoprotein oxidation and its uptake by human macrophages and arterial smooth muscle cells. *Arterioscler. Thromb.* 12, 569–583 (1992).
- Bligh, E. G. & Dyer, W. J. A rapid method of total lipid extraction and purification. *Can. J. Biochem. Physiol.* 37, 911–917 (1959).
- Randle, D. H., Zindy, F., Sherr, C. J. & Roussel, M. F. Differential effects of p19^{Arf} and p16^{Ink4a} loss on senescence of murine bone marrow-derived preB cells and macrophages. *Proc. Natl Acad. Sci. USA* 98, 9654–9659 (2001).
- Stanley, E. R. The macrophage colony-stimulating factor, CSF-1. *Methods Enzymol.* 116, 564–587 (1985).
- Schwenke, D. C. Gender differences in intima-media permeability to low-density lipoprotein at atherosclerosis-prone aortic sites in rabbits. Lack of effect of 17 β -estradiol. *Arterioscler. Thromb. Vasc. Biol.* 17, 2150–2157 (1997).

Acknowledgements

We thank L. Lindgren, C. Ullström and A. Lidell for technical assistance, O. Nerman and K. Wiklander for statistical analysis, D. Schwenke for advice with retention studies, K. Weisgraber for comments on the manuscript, and S. Ordway and G. Howard for editorial assistance. This work was supported by the Swedish Medical Research Council, The Swedish Foundation for Strategic Research, The Swedish Heart-Lung Foundation, and in part by a National Institutes of Health grant.

Competing interests statement

The authors declare that they have no competing financial interests

Correspondence and requests for materials should be addressed to J.B. (e-mail: jan.boren@wlab.gu.se).

T-box gene *tbx5* is essential for formation of the pectoral limb bud

Dae-gwon Ahn^{*†}, Matthew J. Kourakis^{*†}, Laurel A. Rohde^{*†}, Lee M. Silver[†] & Robert K. Ho^{*†}

^{*} Department of Organismal Biology and Anatomy, University of Chicago, Chicago, Illinois 60637, USA.

[†] Department of Molecular Biology, Princeton University, Princeton, New Jersey 08544, USA

The T-box genes *Tbx4* and *Tbx5* have been shown to have key functions in the specification of the identity of the vertebrate forelimb (*Tbx5*) and hindlimb (*Tbx4*)^{1,2}. Here we show that in zebrafish, *Tbx5* has an additional early function that precedes the formation of the limb bud itself. Functional knockdown of zebrafish *tbx5* through the use of an antisense oligonucleotide resulted in a failure to initiate fin bud formation, leading to the complete loss of pectoral fins. The function of the *tbx5* gene in the development of zebrafish forelimbs seems to involve the directed migration of individual lateral-plate mesodermal cells into the future limb-bud-producing region. The primary defect seen in the *tbx5*-knockdown phenotype is similar to the primary defects described in known T-box-gene mutants such as the *spadetail* mutant of zebrafish^{3,4} and the *Brachyury* mutant of the mouse⁵, which both similarly exhibit an altered migration of mesodermal cells. A common function for many of the T-box genes might therefore be in mediating the proper migration and/or changes in adhesive properties of early embryonic cells.

The formation of vertebrate limbs involves a complex series of morphogenetic events, including the specification of limb fields within the lateral-plate mesoderm, induction of the limb buds at appropriate axial levels, and the initiation and patterning of distal limb outgrowth^{6,7}. During early stages of vertebrate limb morphogenesis, *Tbx5* is strongly expressed within the forelimb buds of a variety of vertebrate species^{8–13}. Recent misexpression studies have shown that this gene and a closely related gene, *Tbx4*, which is expressed within the hindlimb bud, are crucial in the determination of limb identity and the regulation of limb outgrowth^{1,2}. However, the initiation of *Tbx5* expression within the anterior lateral-plate mesoderm, which supplies the forelimb progenitor cells, precedes the emergence of visible forelimb buds^{8–11,13}, indicating that this gene might have additional early functions in forelimb development. To investigate the possibility of an earlier function for the *Tbx5* gene during vertebrate forelimb development, we generated a knockdown phenotype in zebrafish, using antisense oligonucleotides containing morpholino moieties in their backbones. These 'morpholino' oligonucleotides are thought to exert their inhibitory effects through physical blocking of the translational initiation of target messenger RNAs, and also have been shown to exhibit a low toxicity and high specificity in a variety of *in vivo* systems¹⁴, including the fertilized eggs of zebrafish¹⁵.

We designed two different morpholino oligonucleotides for the *tbx5* gene of zebrafish, one recognizing the first 25 bases of the coding sequence, the other targeting a sequence of a similar size but located within the 5' untranslated region (UTR), ten nucleotides upstream of the initiation codon. The effectiveness of these oligonucleotides in inhibiting the translation of target mRNAs was first examined by an assay *in vivo* using chimeric mRNAs in which the coding sequence of the gene encoding enhanced green fluorescent protein replaced the coding sequence of *tbx5* in frame after the first 27 bases. Both oligonucleotides were able to block the translation of the green fluorescent protein when injected together with the test mRNA into the early-stage embryo, whereas the control oligonucleotide designed for the 5' UTR sequence of the zebrafish *tbx4* gene